SOME LATTICE CRITERIA FOR PROTON ACCELERATORS AND $p\bar{p}$ COLLIDERS

N Marshall King
Rutherford and Appleton Laboratories, Chilton, Oxon, UK

ABSTRACT

Lattices for 20 TeV proton machines have been surveyed for a wide range of tune values in the range $50 \lesssim Q \lesssim 250$, and their sensitivity to various errors assessed. Results favour lower tunes, in the region of 100, particularly when total quadrupole length and machine circumference are taken into consideration.

1. INTRODUCTION

Lattices considered at the 1978 ICFA Workshop[1] called for tune values in the region of 200 at 20 TeV. However, extrapolation from existing SPS and FNAL tunes according to the scaling law $Q \sim P^{\frac{1}{2}}$ would suggest much lower values in the range Q = 100-150 at 20 TeV.

Further, the 1978 lattices invite the criticism that they involve large numbers of long quadrupoles, with consequent large machine circumference and attendent capital expense. Hence, it seems worthwhile to explore what criteria might be invoked for an optimum choice of tune.

The present exercise concentrates on 20 TeV machines, covers a wide range of tune, $50 \lesssim Q \lesssim 250$, and considers the sensitivity of the normal part of the lattice to various errors in construction and installation. Dipole, quadrupole, and sextupole effects are evaluated according to the formulae of Refs 2 and 3, to 98% probability where appropriate, and conjectured rms error values are assigned.

Basic premises adopted in the 1978 exercise are preserved: namely, FODO cells of about $\pi/2$ phase advance; dipole fields of 10T; quadrupole gradients of about 250T/m; and lattice superperiodicity 8, determined by eight low-β insertions. The insertions are not considered in detail here.

A new approach to the free space allocated for ancillary equipment in the normal cells is adopted, as outlined in Section 2. To compare the different lattices, a consistent selection of working point in the resonance diagrams is made, described in Section 3.

2. LATTICE GEOMETRY

The lattices contain N_B normal FODO cells of about $\mu = \pi/2$ phase advance, with dipole fields B = 10T and quadrupole gradients B' of about 250T/m. A schematic half-cell, involving 'm' dipole units is illustrated below.

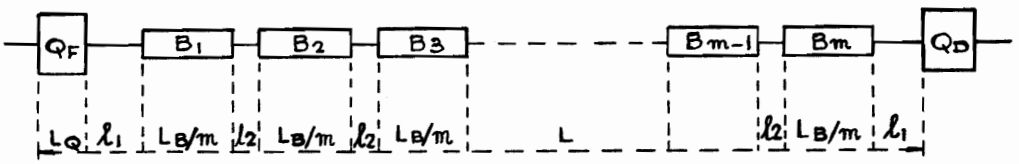

$$L = L_B + L_Q + 2\ell_1 + (m-1)\ell_2$$

Table I

Normal cell lattice parameters for dipole field B = 10T

No. Normal Cells,	N_B	208	304	400	496	592	688	816	912	1008
Tune of Normal Cells,	Q	51.57	75.57	99.57	123.57	167.57	171.57	203.57	227.57	251.57
Tune Shift/Normal Cell,	μ/π	0.4959	0.4972	0.4979	0.4983	0.4985	0.4988	0.4989	0.4991	0.4992
Dipole Length/½-Cell,	L_B(m)	100.76	68.943	52.396	42.255	35.403	30.463	25.684	22.981	20.792
No. Dipoles/½-Cell,	m	14	10	7	6	5	4	4	3	3
Dipole Unit Length,	ℓ_B(m)	7.197	6.894	7.485	7.043	7.081	7.616	6.421	7.660	6.931
Bending Angle/Unit,	ϕ(mrad)	1.079	1.033	1.122	1.056	1.061	1.142	0.9625	1.148	1.039
Total No. Dipoles,	M_B	5824	6080	5600	5952	5920	5504	6528	5472	6048
Total No. Quads,	M_Q	416	608	800	992	1184	1376	1632	1824	2016
Quad Unit Length,	L_Q(m)	3.187	4.398	5.481	6.383	7.179	7.889	8.618	9.173	9.586
Quad Peak Gradient,	B'(T/m)	250.5	253.2	256.0	258.8	261.6	264.5	267.8	270.6	272.9
Half-Cell Length,	L(m)	118.45	85.840	68.875	59.140	52.585	47.851	43.802	41.154	39.379
Circumference Ratio, Normal Cells,	L/L_B	1.1755	1.2451	1.3145	1.3996	1.4853	1.5708	1.7054	1.7908	1.8939
Ring Radius,	R(km)	7.842	8.306	8.769	9.337	9.909	10.479	11.377	11.947	12.635
Ring Circumference,	C(km)	49.275	52.191	55.100	58.667	62.261	65.843	71.485	75.065	79.387
Max Ampl. Function,	β_{max}(m)	402.05	290.77	232.62	199.09	176.44	160.02	145.92	136.66	130.43
Min Ampl. Function,	β_{min}(m)	70.71	51.13	41.05	35.31	31.46	28.70	26.34	24.81	23.78
Max Dispersion Function,	η_{max}(m)	4.89	2.42	1.47	1.02	0.76	0.59	0.45	0.38	0.33
Min Dispersion Function,	η_{min}(m)	2.36	1.17	0.71	0.49	0.37	0.29	0.22	0.19	0.16
Transition γ,	γ_t	47.63	69.84	92.09	114.4	136.7	159.0	188.8	211.2	233.6

To determine cell dimensions, three basic assumptions are made: (i) dipole unit length (L_B/m) is in the region of 7m, consistent with existing technology; (ii) spaces ℓ_1, to accommodate sextupoles, closed orbit correctors, beam sensors, etc. should have a minimum length $\ell_1 \geq 4.0$m; (iii) similarly, inter-dipole spaces ℓ_2 to accommodate pumps, flanges, bellows, electrical connections, etc. should have a minimum length $\ell_2 \geq 0.5$m. These allocations may have to be revised on more detailed scrutiny.

Since $\mu \simeq \pi/2$, the number of normal cells is given by $N_B \simeq 4Q$; and L_B is given by $\pi\rho/N_B$ with $\rho = 6.67128$ km for 20 TeV and B = 10T. Hence, where the subscript 'n.i' stands for 'nearest integer':

$$m = (L_B/7)_{n.i} = (2994/N_B)_{n.i} , \tag{1}$$

and the above assumptions give an upper limit for L_Q in metres:

$$L_Q \leq (L - L_B) - \tfrac{1}{2}(m + 15) . \tag{2}$$

Thin lens analysis[1] with $B' \leq 250$T/m relates L_Q to $\frac{1}{2}$-cell length L:

$$L_Q \geq 377.5/L . \tag{3}$$

Combining (2) and (3), the ratio $L/L_B = R/\rho$ is given by:

$$L/L_B \geq f + (f^2 + 377.5/L_B^2)^{\frac{1}{2}} , \tag{4}$$

$$\text{with } f = 0.25\ (2 + (m+15)/L_B) . \tag{4a}$$

Thus, for a given value of N_B, lattice dimensions are determined for the above minimum values of ℓ_1, ℓ_2, with maximum quadrupole gradient B = 250T/m to thin lens approximation.

3. WORKING POINT

The typical superperiod resonance diagram for S = 8 is illustrated in Fig 1, where all superperiod resonances to 3rd order are shown as solid lines, and 4th order as serrated lines. An exception is the 2nd order difference line $Q_x - Q_y = 0$, shown serrated. For clarity, Q values are exemplified by the weak-focusing case $Q_o = 52$, where Q_o is the nominal tune giving a precise $\mu = \pi/2$ phase advance per cell: (ie. $Q_o = N_B/4$).

The $\frac{1}{4}$-integer square and working point picked out in Fig 1 is reasonably far from dangerous systematic lines, and has been chosen to typify all the lattices compared here. It is expanded in Fig 2 to show neighbouring error resonances to 4th order, again taking the $Q_o = 52$ case as an example. The working point at $Q_o - 0.43$ is shown at the centre of a circle, radius $\Delta Q = 0.02$ to give a feeling for the scale. The resulting phase advance per normal cell is given by $\mu/\pi = 0.5 - 0.215/Q_o$, always close to $\mu = \pi/2$.

4. LATTICE PARAMETERS

With lattice geometry chosen according to Section 2, and working points according to Section 3, lattice parameters for the range $52 \leq Q_o \leq 252$ are listed in Table I.

The lattice functions were calculated originally using thin lens formulae[1], and were checked subsequently by an accurate matrix program[4]. As in the 1978 study, results are in good agreement, the chief difference being an underestimate of quadrupole strengths in the thin-lens approach: by 0.2% at $Q_o = 52$, increasing to about 9% at $Q_o = 252$. The accurate computed values are quoted in Table I.

5. CLOSED ORBIT DEVIATIONS

Starting from the formulae of Ref 2, pp 23-24, approximate expressions for maximum closed orbit deviations to 98% probability are derived for the various types of error. The approximation consists in taking β-values in the dipoles and drift spaces to be the rough average value $\frac{1}{2}(\beta_{max} + \beta_{min})$.

5.1 Random Errors in Dipole Field

The maximum horizontal deviation due to random field errors (ΔB/B) rms is given by:

$$\hat{x}_{\Delta B} \approx \frac{2.4\pi}{\sqrt{2}} \left[\frac{1+{}^1/_3|\mathrm{Sin}\pi Q|}{|\mathrm{Sin}\pi Q|} \right] \left[\frac{\beta_{max}(\beta_{max} + \beta_{min})}{M_B} \right]^{\frac{1}{2}} \left(\frac{\Delta B}{B}\right)_{rms} , \qquad (5)$$

where $M_B = 2m\, N_B$ is the total number of dipoles. Since all the lattices have a tune value given by an odd integer + 0.57, Equation (5) reduces to:

$$\hat{x}_{\Delta B} \approx 7.24 \left[\beta_{max} (\beta_{max} + \beta_{min})/M_B \right]^{\frac{1}{2}} . (\Delta B/B)_{rms} . \qquad (5a)$$

5.2 Random Dipole Tilts

Similarly, the maximum vertical deviation due to random dipole tilts $(\Delta\theta)_{rms}$ is given by:

$$\hat{y}_\theta \approx 7.24 \left[\beta_{max}(\beta_{max} + \beta_{min})/M_B \right]^{\frac{1}{2}} . (\Delta\theta)_{rms} . \qquad (6)$$

5.3 Random Quadrupole Displacements

Denoting the rms quadrupole displacements by $(\Delta q)_{rms}$ for either the x or y planes,

$$\hat{x}_{\Delta q} = \hat{y}_{\Delta q} \approx \frac{1.2}{\sqrt{2}} \left[\frac{1 + {}^1/_3|\mathrm{Sin}\pi Q|}{|\mathrm{Sin}\pi Q|} \right] \left[\beta_{max}(\beta_{max} + \beta_{min}).M_Q \right]^{\frac{1}{2}} KL_Q.(\Delta q)_{rms} , \qquad (7)$$

where $M_Q = 2N_B$ is the total number of quadrupoles of length L_Q and gradient factor K.

For 20 TeV and 250 T/m, $K = 3.7474 \times 10^{-3}$, so that:

$$\hat{x}_{\Delta q} = \hat{y}_{\Delta q} \approx 4.318 \times 10^{-3} \left[\beta_{max}(\beta_{max} + \beta_{min}).M_Q \right]^{\frac{1}{2}} . L_Q . (\Delta q)_{rms} . \qquad (7a)$$

5.4 Stray Field in Normal Lattice Drift Spaces

Denoting the rms vertical and horizontal stray fields by $(\Delta B_{sy})_{rms}$ and $(\Delta B_{sx})_{rms}$, the factor $|2N_B \{2\ell_1^2 + (m-1)\ell_2^2\}|^{\frac{1}{2}}$ arises in the formulae. Using the values $\ell_i = 4.0$m and

ℓ_2 = 0.5m chosen in Section 2, the approximate expressions become:

$$\left|\begin{matrix}\hat{x}_{\Delta Bs}\\ \hat{y}_{\Delta Bs}\end{matrix}\right| \approx 0.6\left[\frac{1+1/3|\mathrm{Sin}\pi Q|}{|\mathrm{Sin}\pi Q|}\right]\left[\beta_{max}(\beta_{max}+\beta_{min}).(m+127)N_B\right]^{\frac{1}{2}}\frac{1}{\rho B_{inj}}\left|\begin{matrix}(\Delta B_{sy})_{rms}\\ (\Delta B_{sx})_{rms}\end{matrix}\right| . \qquad (8)$$

Choosing an injection field B_{inj} = 2.5 x 10^3G, these reduce to:

$$\left|\begin{matrix}\hat{x}_{\Delta Bs}\\ \hat{y}_{\Delta Bs}\end{matrix}\right| \approx 4.886 \times 10^{-8}\left[(m+127)N_B\ \beta_{max}(\beta_{max}+\beta_{min})\right]^{\frac{1}{2}}\left|\begin{matrix}(\Delta B_{sy})_{rms}\\ (\Delta B_{sx})_{rms}\end{matrix}\right| . \qquad (8a)$$

5.5 Summary of Closed Orbit Deviations

As was the case for lattice parameters, these estimates of closed orbit deviations have been checked using an accurate matrix tracking program[4], with results in good agreement. The accurate computed values are quoted in Tables II and III, scaled to conjectural values of rms errors in general agreement with SPS experience, but modified to account for uncertainties in superconducting magnet performance. In each plane, the effects have been added in quadrature to give final estimates $(\hat{x})_{rms}$, $(\hat{y})_{rms}$. These values are plotted in Fig 3.

Clearly, the deviations are dominated by quadrupole misalignments at the higher tune values. Although the precise form of the Fig 3 curves depends very much on the chosen rms values of the field and quadrupole errors, the indication is that a Q value in the region of 100 would be a sensible choice.

6. TUNE SHIFTS AND RESONANCE WIDTHS

6.1 Random Errors in Quadrupole Gradient

Random errors in quadrupole gradient $(\Delta B'/B')_{rms}$ contribute to the width of the half integer resonances in the neighbourhood of the working point. To good accuracy, the contribution to full width is given by:

$$\Delta Q_q \approx \frac{1}{2\pi} KL_Q \left[N_B\left(\beta_{max}^2+\beta_{min}^2\right)\right]^{\frac{1}{2}}\left(\Delta B'/B'\right)_{rms} . \qquad (9)$$

6.2 Random Gradient Errors in Dipoles

The contribution from gradient errors $(\Delta B'_{dip})_{rms}$ in the dipoles may be expressed, to less good accuracy, by:

$$\Delta Q_B \approx \frac{(\beta_{max}+\beta_{min})}{2M_B^{\frac{1}{2}}} . \frac{(\Delta B'_{dip})_{rms}}{B} , \qquad (10)$$

where, as in Section 5, all dipoles are assumed to have a rough average β-value given by $\frac{1}{2}(\beta_{max}+\beta_{min})$.

6.3 Resultant Width of Half-Integer Resonances

Table IV lists these two effects for conjectural values of the rms errors. In the case

Table II

Horizontal Closed Orbit Deviations (mm)

$(\Delta B/B)_{rms} = 10^{-3}$, $(\Delta q_x)_{rms} = 0.15$ mm, $(\Delta B_{sy})_{rms} = 0.28G$, $B_{inj} = 2.5$ kG

N_B	208	304	400	496	592	688	816	912	1008
$\hat{x}_{\Delta B}$	37.6	26.5	22.1	18.3	16.2	15.3	12.8	13.1	11.9
$\hat{x}_{\Delta q}$	18.4	22.4	25.9	29.0	31.8	34.7	38.0	40.6	42.9
$\hat{x}_{\Delta Bsy}$	1.0	0.9	0.8	0.8	0.7	0.7	0.7	0.7	0.7
$(\hat{x})_{rms}$	41.9	34.7	34.1	34.3	35.7	37.9	40.1	42.7	44.5

Table III

Vertical Closed Orbit Deviations (mm)

$(\Delta q_y)_{rms} = 0.15$ mm, $(\Delta\theta)_{rms} = 2\times10^{-4}$rad, $(\Delta B_{sx})_{rms} = 0.11G$, $B_{inj} = 2.5$kG

N_B	208	304	400	496	592	688	816	912	1008
$\hat{y}_{\Delta q}$	18.4	22.4	25.9	29.0	31.8	34.7	38.0	40.6	42.9
$\hat{y}_{\Delta\theta}$	7.5	5.3	4.4	3.7	3.2	3.0	2.6	2.6	2.4
$\hat{y}_{\Delta Bsx}$	0.4	0.4	0.3	0.3	0.3	0.3	0.3	0.3	0.3
$(\hat{y})_{rms}$	19.9	23.0	26.3	29.2	32.0	34.8	38.1	40.7	43.0

Table IV

Half Integer Resonance Widths

$(\Delta B'/B')_{rms} = 10^{-3}$, $(\Delta B'_{dip})_{rms}/B = 10^{-2}$ m^{-1}

N_B	208	304	400	496	592	688	816	912	1008
ΔQ_q	0.011	0.014	0.016	0.018	0.019	0.020	0.022	0.024	0.024
ΔQ_B	0.031	0.022	0.018	0.015	0.014	0.013	0.011	0.011	0.010
$(\Delta Q)_{rms}$	0.033	0.026	0.024	0.023	0.024	0.024	0.025	0.026	0.026

of quadrupole gradient errors, the value $(\Delta B'/B')_{rms} = 10^{-3}$ seems to be a reasonable aim: gradient errors in superconducting dipoles pose more of a problem. Here, the suggested value $(\Delta B'_{dip})_{rms}/B = 10^{-2}$ m^{-1} corresponds, for example, to a field error $\Delta B/B = 0.5\times10^{-3}$ at the edge of a 5 cm radius aperture, ascribed to linear gradient error and which is evaluated at an injection field of 2.5 kG.

Adding the two effects in quadrature, an estimate $(\Delta Q)_{rms}$ is listed in Table IV. This suggests a minimum value in the region Q = 100-150: as before it should be emphasised that much depends on the precise choice of rms error values. Nevertheless, it is

encouraging to derive a value consistent with the arguments of Section 5.

6.4 Sextupolar Field Errors in Dipoles

In Ref. 3, effects due to sextupole field components in straight dipoles were analysed. Since such terms are likely to be large in superconducting magnets, it seems prudent to evaluate their effects. Expressing the dipole field across the aperture by:

$$B = B_o\left[\, 1 + b_1 x + b_2 x^2 + \ldots\ldots \,\right] \quad , \tag{11}$$

the b_1 term used above was 10^{-2} m^{-1}. Turning to the b_2 term, an estimate based on FNAL superconducting dipoles[5] relates to a sextupole field of about 5G at 2.5 cm radius for a design field B_o = 5 kG: that is, $b_2 = 1.6$ m^{-2}. This is about 4 times the corresponding value for SPS conventional magnets.

Due to closed orbit curvature in the sextupolar field, first order tune shifts arise in the x and y planes, given by

$$\Delta Q = \frac{1}{2\pi\rho} \int_o^{C} \frac{1}{2}\, b_2 c_1 . \beta_{dip} ds, \tag{12}$$

where c_1 is the error in x-position of the closed orbit at entrance to a dipole, compared with an ideal position. Taking c_1 to be random with an rms value of 0.2mm, Equation 12 leads to an expression directly comparable with Equation 10. The contribution to the full width of the half integer resonances is then:

$$\Delta Q \approx \frac{\left(\beta_{max} + \beta_{min}\right)}{2M_B^{\frac{1}{2}}} \; . \; 3.2 \times 10^{-4} \quad , \tag{12a}$$

where the factor 3.2×10^{-4} is to be compared with the value 10^{-2} used in Equation 10. Hence this effect may safely be neglected.

Turning to the second order tune spreads directly attributable to the sextupolar field term, Equations 48 & 51 of Ref. 3 allow the effects to be estimated. These relations simplify considerably, taking $Q_x = Q_y = Q$, $c_2 \approx 1$, and constant values of $\beta = \bar{\beta}$ in all dipoles:

$$\begin{aligned} \Delta Q_{2x} &\approx -\frac{5}{12}\, b_2^2\, \bar{\beta}_x^3 \frac{\varepsilon_x}{Q} + b_2^2\left(\tfrac{1}{2}\bar{\beta}_x^2\bar{\beta}_y - \frac{1}{3}\,\bar{\beta}_x\bar{\beta}_y^2\right)\frac{\varepsilon_y}{Q} \\ \Delta Q_{2y} &\approx -\frac{5}{12}\, b_2^2\, \bar{\beta}_x\bar{\beta}_y^2 \frac{\varepsilon_y}{Q} + b_2^2\left(\tfrac{1}{2}\bar{\beta}_x^2\bar{\beta}_y - \frac{1}{3}\,\bar{\beta}_x\bar{\beta}_y^2\right)\frac{\varepsilon_x}{Q} \end{aligned} \tag{13}$$

Making the further simplifying assumptions $\bar{\beta}_x = \bar{\beta}_y = \bar{\beta} = \frac{1}{2}\left(\beta_{max} + \beta_{min}\right)$ and $\varepsilon_x = \varepsilon_y = \varepsilon = 3 \times 10^{-5} m/\beta\gamma$, the expressions become:

$$\Delta Q_{2x} = \Delta Q_{2y} \approx -\frac{1}{4}\, b_2^2\, \bar{\beta}^3\, \varepsilon/Q \tag{13a}$$

Evaluating the effects at $\gamma_{inj} = 500$, with $b_2 = 1.6$ m^{-2} as before:

Table V

Second Order Tune Spreads

N_B	208	304	400	496	592	688	816	912	1008
$\Delta Q_2 \times 10^{-3}$	9.8	2.5	1.0	0.5	0.3	0.2	0.1	0.09	0.07

Thus although the spreads could be important at very low tune values, they have fallen to about 10^{-3} at $Q \approx 100$.

It should also be remarked that the tune spreads will be much more markedly affected by the lumped sextupole elements inserted for chromatic correction. These have not been considered here.

7. CONCLUSIONS

Surveying FODO lattices for 20 TeV proton rings over a wide range of tune values, the effects of closed orbit deviations, half-integer resonance widths, and sextupolar effects in the dipoles have been examined. The results all seem to favour a choice of normal lattice tune in the neighbourhood of Q = 100. This is in good agreement with a $P^{\frac{1}{2}}$ scaling from existing SPS and FNAL lattices.

Apart from such criteria, the likely cost of going to higher tune values may be envisaged from a glance at Table I: not only the numbers of quadrupoles, but their lengths, increase with tune value, as does the ring circumference.

It should also be remarked that, if the envisaged closed orbit deviations are to be completely accommodated in the vacuum chamber before correction, the magnet apertures should be about the same dimension as in existing proton machines, - this despite the fact that the beam radius should never be greater than a fraction of a millimetre. After correction, the beam should lie completely in a very good field region.

ACKNOWLEDGEMENT

The author wishes to thank J R M Maidment for checking the lattice calculations with his matrix tracking program, as mentioned in the text.

* * *

REFERENCES

1) E Keil & N M King. Proc. ICFA Workshop on Possibilities and Limitations of Accelerators and Detectors. FNAL (1978).

2) C Bovet et al. A Selection of Formulae and Data Useful for the Design of AG Synchrotrons. CERN/MPS-SI/Int.DL 70/4 (1970).

3) N M King & M Cornacchia. Sextupolar Tune Shifts in the SPS. CERN LabII-DI-PA/74-1(1974).

4) J R M Maidment. Private communication.

5) A Tollestrup. Private communication.

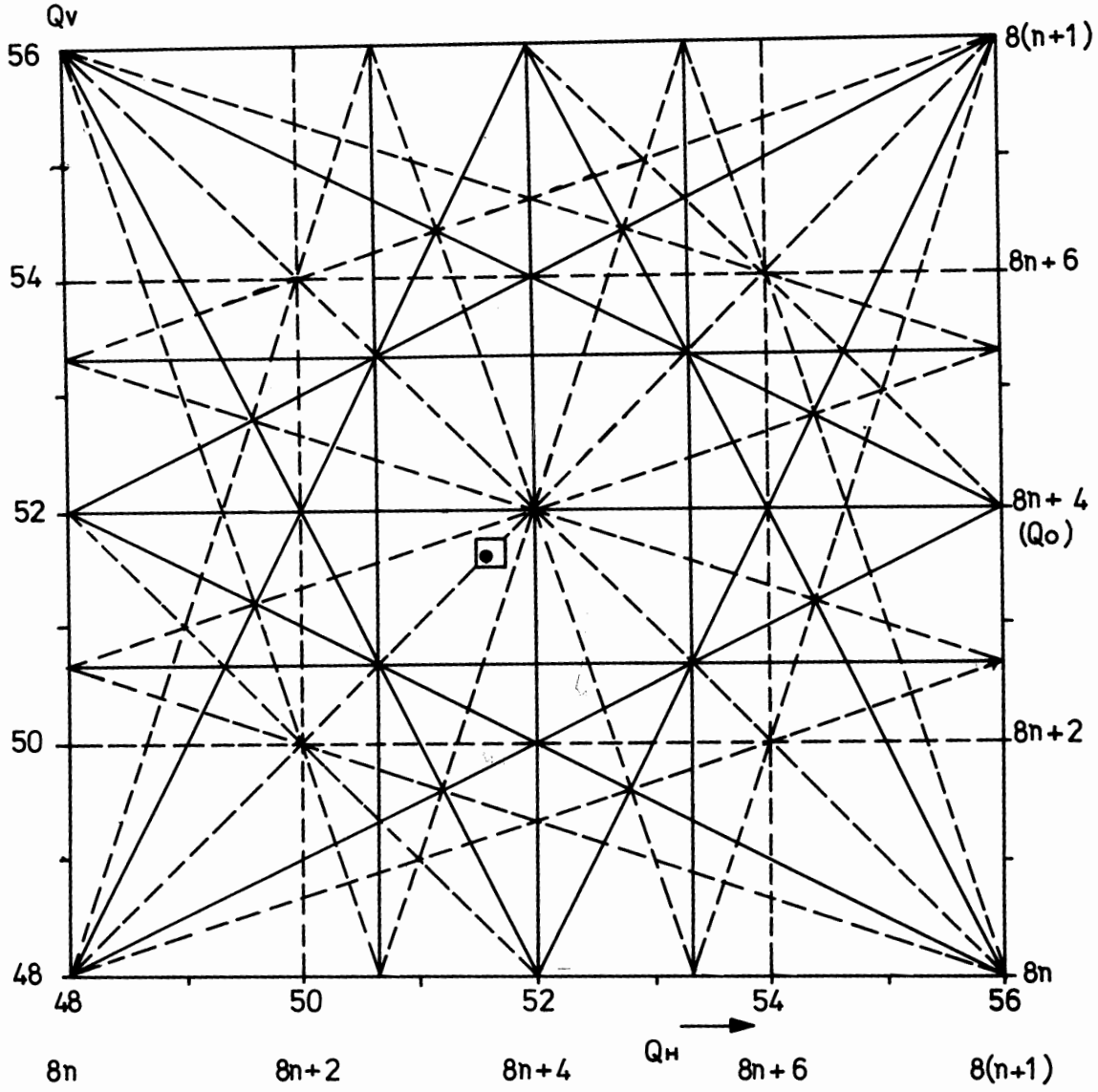

FIG 1 Superperiod Resonances to 4th Order
$S = 8$, $N_B = 4Q_o$

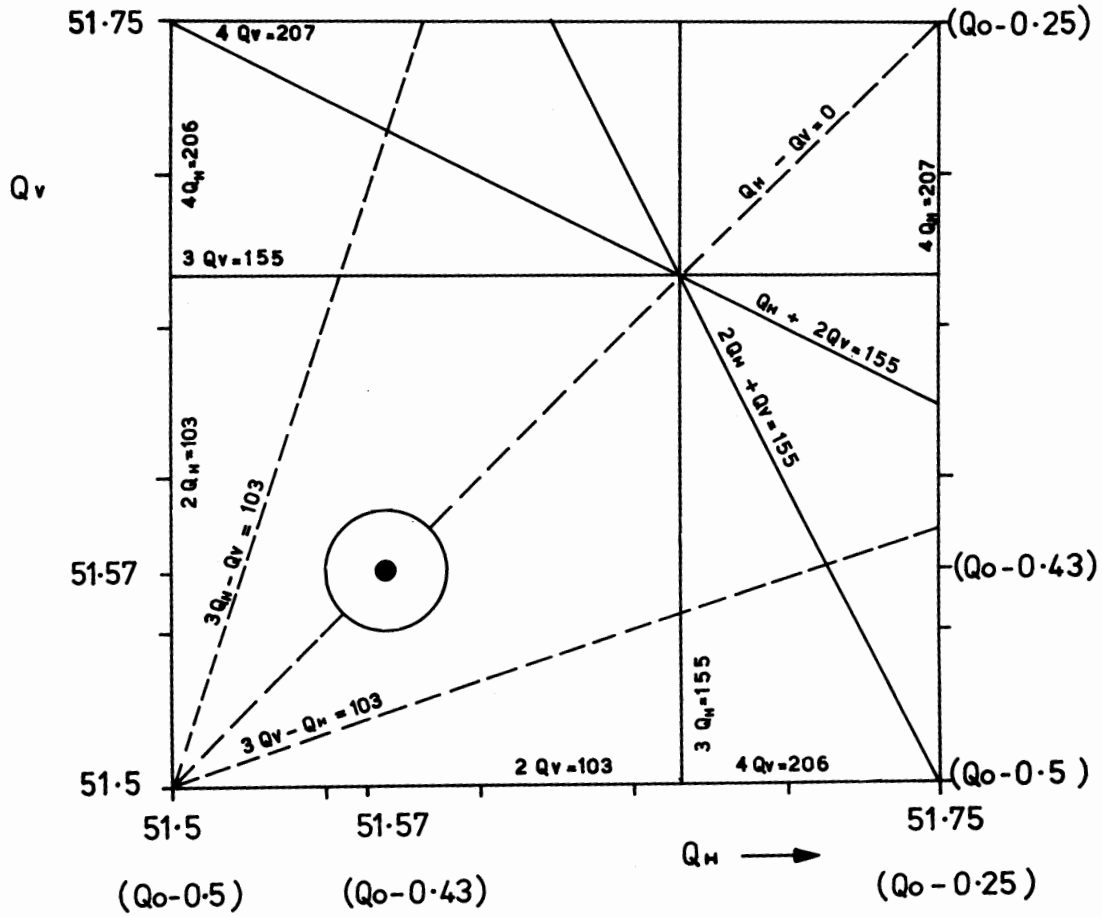

FIG 2 Error Resonances in ¼-Integer Square
Working Point $Q_H = Q_V = Q_o - 0.43$

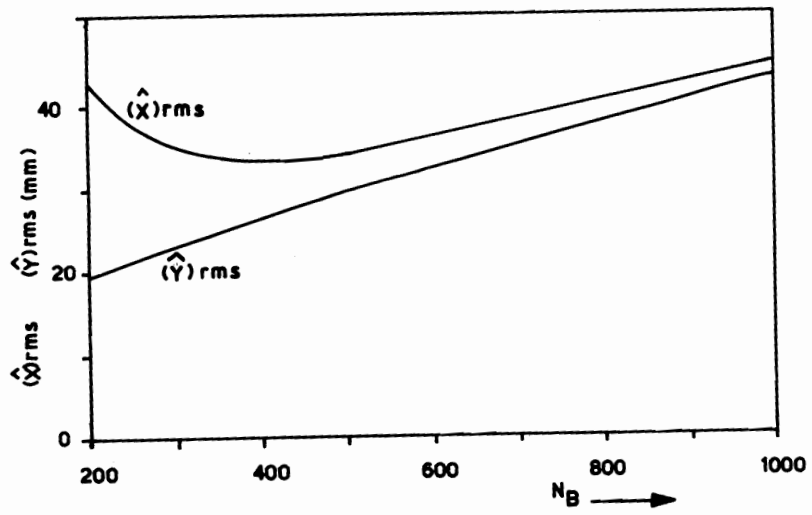

FIG 3 Estimated Closed Orbit Deviations to 98% Probability versus Number of Normal Cells $N_B \approx 4Q$